Available online at www.sciencedirect.com

ScienceDirect

Procedia Structural Integrity 2 (2016) 2076–2083

Structural Integrity Procedia

www.elsevier.com/locate/procedia

21st European Conference on Fracture, ECF21, 20-24 June 2016, Catania, Italy

The Heat Energy Dissipated in a Control Volume to Correlate the Fatigue Strength of Bluntly and Severely Notched Stainless Steel Specimens

Giovanni Meneghetti*, Mauro Ricotta, Bruno Atzori

Department of Industrial Engineering, University of Padova, via Venezia, 1, 35131 Padova, Italy

Abstract

In previously published papers by the authors, the specific heat energy loss per cycle (the Q parameter) was used to rationalize about 120 experimental results generated from constant amplitude, push-pull, stress- or strain-controlled fatigue tests on plain and notched hot rolled AISI 304 L stainless steel specimens as well as from cold drawn un-notched bars of the same steel, tested under fully-reversed axial or torsional fatigue loadings. It has been shown that Q can be estimated starting from the cooling gradient measured at the critical point immediately after the fatigue test has been stopped. Concerning notched specimens, it was noted that a 3 mm notch tip radius was close to the limitation of applicability of the adopted temperature sensor, consisting in 0.127-mm-diameter thermocouples, because of the 1.5-to-2 mm diameter spot of the glue which prevented to measure the maximum temperature level. In this paper, the fatigue-damage-index effectiveness of Q parameter was investigated, carrying out fully reversed axial fatigue tests on 4-mm-thick AISI 304L specimens, having 3, 1 and 0.5 mm notch tip radii. The cooling gradients were measured by using an infrared camera, characterized by a 20 μm/pixels spatial resolution. As a result, all new fatigue data could be rationalized using the same scatter band published previously by the authors.

Peer-review under responsibility of the Scientific Committee of ECF21.

Keywords: heat energy loss per cycle; energy methods; AISI 304L; fatigue; notch effect; thermography.

* Corresponding author. Tel.: +0039-049-827-6751; fax: +0039-049-827-6785.
E-mail address: giovanni.meneghetti@unipd.it

Peer review under responsibility of the Scientific Committee of ECF21.
10.1016/j.prostr.2016.06.260

1. Introduction

During fatigue loading of metallic materials, some mechanical energy is expended to induce plastic deformations. Of the total energy expended in a unit volume of material, only part is accumulated in the form of internal energy and is responsible for fatigue damage accumulation and final fracture. The remaining part is dissipated as heat (Ellyin, 1997), which induces some temperature increase during fatigue testing. Temperature is a manifestation of the thermal energy dissipation and it has been used in fatigue-related studies, such as the rapid engineering estimation of the fatigue limit of metallic materials and components by Dengel et al (1980), Curti et al (1989), Luong (1995), La Rosa and Risitano (2000), Curà et al (2005), the damage detection and propagation in metal materials and structures as well as composites by Reifsnider and Williams (1974), Plekhov et al (2005), Ummenhofer and Medgenberg (2009), Jones et al (2010) and more recently the analysis of fatigue life under constant amplitude by Fargione et al (2002), Starke et al (2007), Jegou et al (2013), and block loading by Fang et al (2012), Risitano and Risitano (2013). However, the temperature level which the material attains in a fatigue test depends on the thermal and mechanical boundary conditions and is such that the thermal energy per cycle "generated" in response to the given load cycle is dissipated to the surroundings. Therefore, the thermal energy dissipated in a unit volume of material per cycle (the parameter Q) has been adopted recently as a fatigue damage indicator during fatigue tests of stainless steel specimens by Meneghetti (2007). A relatively simple experimental technique has also been proposed to estimate Q from in-situ measurements of the temperature at the surface of a specimen or a component, starting from the cooling gradient measured at the point to be assessed immediately after the fatigue test has been stopped:

$$Q = -\frac{\rho \cdot c \cdot \partial T / \partial t}{f} \tag{1}$$

where T(t) is the time-variant temperature at a point, ρ is the material density, c is the material specific heat and f is the load test frequency applied before the test interruption. The specific energy Q is a material property for a given load cycle (defined by amplitude and mean values), which can be assumed as a fatigue damage parameter similarly to the plastic strain hysteresis energy (Ellyin, 1997).

Recently, the Q parameter was adopted to rationalize about 120 experimental results generated from constant amplitude, push-pull, stress- or strain-controlled fatigue tests on plain and notched hot rolled AISI 304 L stainless steel specimens by Meneghetti and Ricotta (2012), Meneghetti et al (2013), as well as from cold drawn un-notched bars of the same steel tested under fully-reversed axial or torsional fatigue loadings by Meneghetti et al (2014). Notched specimens had either lateral U- or V- notches, with root radii equal to 3 or 5 mm, or a central hole with radius equal to 8 mm. Fig 1 shows all fatigue test results in terms of net-section stress amplitude σ_{an} or τ_a, the mean fatigue curves and the 10%-90% survival probability scatter bands. The figure reports also the inverse slope k of the curves, the stress-based scatter index $T_\sigma=\sigma_{a,10\%}/\sigma_{a,90\%}$ (T_τ) and the life-based scatter index $T_{N,\sigma}$ ($T_{N,\tau}$). In the case of strain-controlled fatigue tests, the stress amplitude reported in Fig.1 is the value that was measured at half the fatigue life. To apply the energy method, temperature was monitored during the fatigue tests in the gauge section of plain specimens or at the root of notched specimens. In the former case an infrared camera or thermocouples were adopted, while in the latter case only thermocouples were used. According to Eq. (1), the specific heat loss Q was determined during each fatigue test and it was seen to be fairly constant. By taking the value at half the fatigue life, Fig.2 shows the same data reported in Fig. 1 re-analysed in terms of the Q parameter, where the 10%-90% scatter band shown in the figure was fitted only on the fatigue data published by Meneghetti et al (2013). However, Fig. 2 shows that the additional data obtained under axial and torsional fatigue tests by Meneghetti et al (2014) can be interpreted by the same scatter band. One can note that in Fig. 2 some of the V-notch experimental data fall below the energy-based scatter band. Meneghetti et al (2013) pointed out that this result might suggest that for this material 3 mm notch radius is close to the limitation of practical applicability of the adopted thermocouples, having 0.127 mm wire diameter. In fact, due to the thermocouples' size as well as to the extension of the area covered by the adhesive (about 1.5–2mm in diameter), the accuracy of the adopted thermocouple sensors to evaluate locally the energy Q becomes critical. Therefore, the local value of the dissipated energy density per cycle is averaged over an area too large with respect to the gradient of the stress/strain field induced by the notch radius.

The aim of this paper is to analyse the fully reversed axial fatigue behaviour of notched AISI 304L stainless steel

specimens, characterized by notch radii equal to 0.5-, 1- and 3-mm, in terms of the Q parameter, which has evaluated by means of an infrared camera allowing for a higher spatial resolution. As a result, all new fatigue data were rationalized by the same energy-based fatigue scatter band previously proposed by Meneghetti et al. (2013).

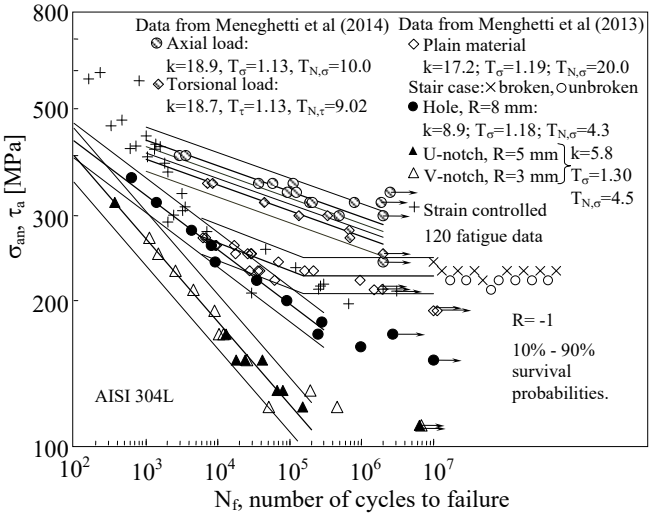

Fig. 1. Completely reversed axial and torsional fatigue test results relevant to AISI 304L steel specimens analysed in terms of net section stress amplitude (from Meneghetti et al. (2014)).

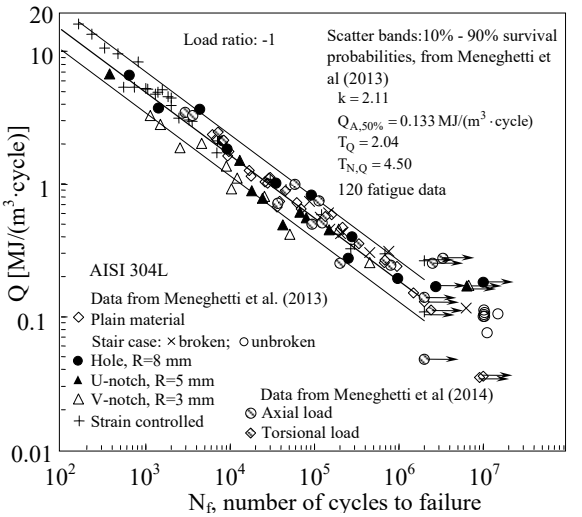

Fig. 2. Fatigue data reported in Fig. 1 analysed in terms of specific heat loss per cycle. Scatter band is defined for 10% and 90% survival probabilities (from Meneghetti et al. (2014)).

2. Material, specimens' geometry and test conditions

Constant amplitude, push-pull, stress controlled fatigue tests were carried out on specimens prepared from 4-mm-thick hot rolled AISI 304L stainless steel sheets, according to the geometry shown in Fig. 3. Some mechanical properties of tested material (engineering proof stress $R_{p0.2}$, engineering tensile strength R_m, elongation at break A%) are listed in Table 1.

3D linear elastic finite element analyses were carried out to calculate the net-section stress concentration factor, K_{tn}, of specimens shown in Fig.3c, which resulted K_{tn} =4.26, 7.39 and 8.96 for R=3, 1 and 0.5 mm, respectively.

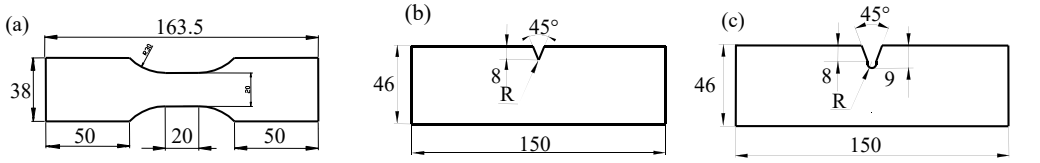

Fig. 3. Specimen's geometry for a) plain, b) severely (R=0.1, 0.5 mm)- and c) blunt notched specimens (R= 1 and 3 mm).

All fatigue tests were carried out by using a servo-hydraulic Schenck Hydropuls PSA 100 machine equipped with a 100 kN load cell and a Trio Sistemi RT3 digital controller. Plain specimens were tested to evaluate the material stress-life curve as well as the fatigue limit, $\sigma_{A,-1}$, by means of a short stair case procedure at 10 million cycles. Specimen's temperature was measured by using copper-constantan thermocouple wires having diameter 0.127 mm, which were fixed at the specimen's centre by means of a silver-loaded conductive epoxy glue. Temperature signals generated by the thermocouples were acquired by means of a data logger Agilent Technologies HP 34970A operating at a maximum sample frequency, f_{acq}, of 22 Hz (accuracy equal to 0.02 °C). Load test frequencies between 3 and 25 Hz were adopted depending on the applied stress level. In order to limit the stabilized temperature observed during the fatigue tests below 70°C, a blower was used to cool the specimens. About ten minutes before each cooling, the blower was switched off. At the same time the test frequency was appropriately reduced in order to

maintain the same surface temperature level. After that, the fatigue test was suddenly stopped to measure the cooling gradient, in order to apply equation (1).

Regarding the notched specimens, after machining 38 x 163.5 mm rectangular sheets, their surfaces were polished by using progressively finer emery papers, namely starting from grade 100 up to grade 4000. Then notches were obtained by wire electro discharge machining, followed by electrochemical polishing. Finally, a black paint was applied to the specimens' surface to increase the emissivity. Surface temperature was monitored by using a FLIR SC7600 infrared camera, having a 1.5-5.1 μm spectral response range, 50 mm focal lens, a noise equivalent temperature difference (NETD) < 25 mK, an overall accuracy of 0.05°C, operating at a frame rate, f_{acq}, equal to 200 Hz and equipped with an analog input interface, which was used to sample synchronously the force signal coming from the load cell. To increase the infrared camera spatial resolution, a 30 mm extender ring was adopted, which allowed a spatial resolution ranging from 20 to 23 μm/pixel, depending on the distance between the specimen's surface and the focal lens. Due to the extender ring, the Field of View (FoV) was reduced to 320x256 pixels, which corresponds to a minimum of 6.4 mm x 5.1 mm and a maximum of 7.4 mm x 5.9 mm.

Severely notched specimens, having 0.1 mm notch radius, were tested to evaluate the threshold range value of the mode I stress intensity factor, ΔK_{th}, by means of a short stair case procedure at 10 million cycles. In this case, a load test frequency equal to 37 Hz was adopted. Regarding the fatigue tests carried out on R=0.5, 1 and 3 mm, test frequencies ranged from 5 to 30 Hz, depending on the applied stress amplitude.

Table 1. Mechanical properties of 4-mm-thick hot rolled AISI 304L stainless steel.

$R_{p0.2}$ (*MPa*)	R_m (*MPa*)	A (*%*)	$\sigma_{A,-1}$ (*MPa*)	ΔK_{th} ($MPa \cdot m^{0.5}$)	a_0 (*mm*)
279	620	57.0	202	8.69	0.147

Crack nucleation at the notch tip was monitored by using AM4115ZT Dino-lite digital microscope having a magnification ranging from 20X up to 220X. The infrared camera and the travelling microscope monitored the opposite surfaces of the specimens.

3. Fatigue test results in terms of net stress amplitude

Fatigue test results are summarized in Fig. 4 in terms of the applied net stress amplitude σ_{an} and compared to those published by Meneghetti et al (2013) for a 6-mm-thick hot rolled made of AISI 304L. The figure reports the mean curves, the 10%-90% survival probability scatter bands, the inverse slope k, the reference fatigue strength $\sigma_{A,50\%}$ evaluated at N_A= 2 million cycles with 50% survival probability, and the stress- as well as the life-based scatter index T_σ and $T_{N,\sigma}$, respectively. The experimental data were statistically analyzed under the hypothesis of log-normal distribution of the number of cycles to failure with a 95% confidence level. It is seen that the material analyzed in the present work is characterized by a lower fatigue limit, $\sigma_{A,-1,}$ (202 MPa < 225 MPa) and that the sharper notches tested in the present paper have a slightly lower fatigue strength.

Finally, the short stair case procedure carried out on severely notched specimens gave ΔK_{th}=8.69 $MPa \cdot m^{0.5}$. Then the material length parameter, a_0, proposed by El Haddad et al. (1979) resulted 0.147 mm, according to Eq. (2):

$$a_0 = \frac{1}{\pi} \cdot \left(\frac{\Delta K_{th}}{2 \cdot \sigma_{A,-1}} \right)^2 \tag{2}$$

According to previous observations (Meneghetti et al (2013)), Fig. 4a shows that, although K_{tn} is equal to 4.26, 7.39 and 8.96 for specimens having notch radius equal to 3, 1 and 0.5 mm, respectively, the fatigue strength reduction factor is only 2.23. As a conclusion, Fig. 4a demonstrates that neither net-section nor linear elastic peak stresses are able to rationalize the fatigue behavior of the specimens tested in this paper.

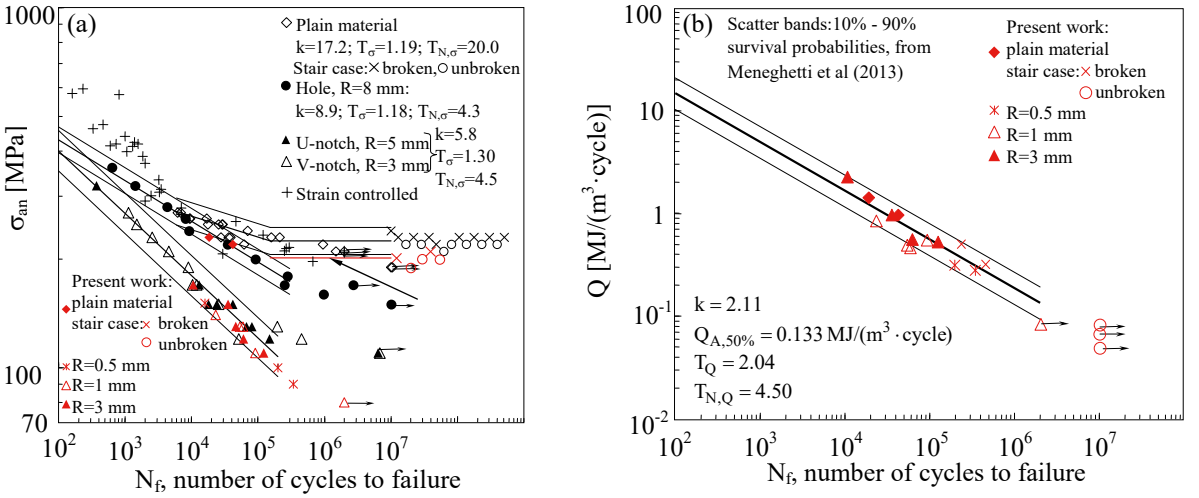

Fig. 4. Results of new fatigue tests in terms of a) applied net stress amplitude and b) specific heat loss per cycle. Scatter band is defined for 10% and 90% survival probabilities (from Meneghetti et al. (2013)).

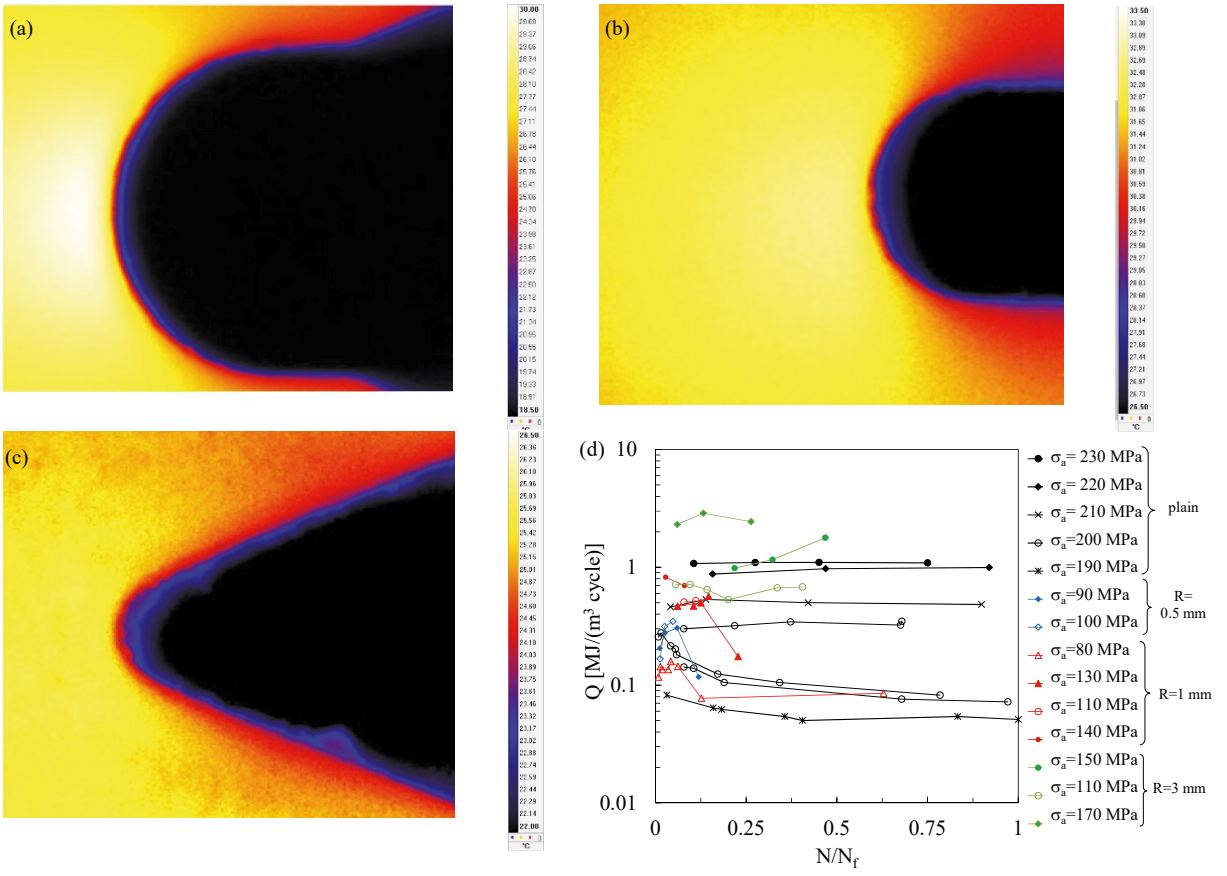

Fig. 5. Example of temperature maps for a) R=3 mm (σ_a=110 MPa, N_f=122659, f=20 Hz), b) R=1 mm (σ_a=110 MPa, N_f=90970, f=20 Hz), c) R=0.5 mm notch radius (σ_a=100 MPa, N_f=198632, f=30 Hz) and d) Q versus N/N_f trends, measured during the fatigue tests.

4. Energy-based synthesis of fatigue test results

During each fatigue test, several stops were made in order to estimate the energy parameter Q and its evolution during the fatigue life, by using the cooling gradient technique according to Eq. (1). Fig. 5a-c show some examples of temperature maps measured during the fatigue test just before the test stop. Fig.5d shows the Q evolution versus the number of cycles N, normalized with respect to the N_f. It can be observed that for plain specimens Q is practically constant during the fatigue life, while in the case of notch specimens the measurements of Q were suspended after the crack initiation had occurred.

Fig. 6 shows some characteristic examples of cooling curves in the case of plain specimens (Fig. 6a), and those relevant to the specimens shown in Fig. 5a-c for R= 3 mm (Fig. 6b), R=1 mm (Fig. 6c) and R=0.5 mm notch radius (Fig. 6d), respectively. In all cases, before test interruption at time t=t* temperature oscillates due to the thermoelastic effect, which is superimposed to mean temperature signal. Concerning the plain specimens, Fig. 6a shows that after t=t* the time window useful to calculate the cooling gradient is on the order of some seconds and the corresponding temperature variations are on the order of one degree.

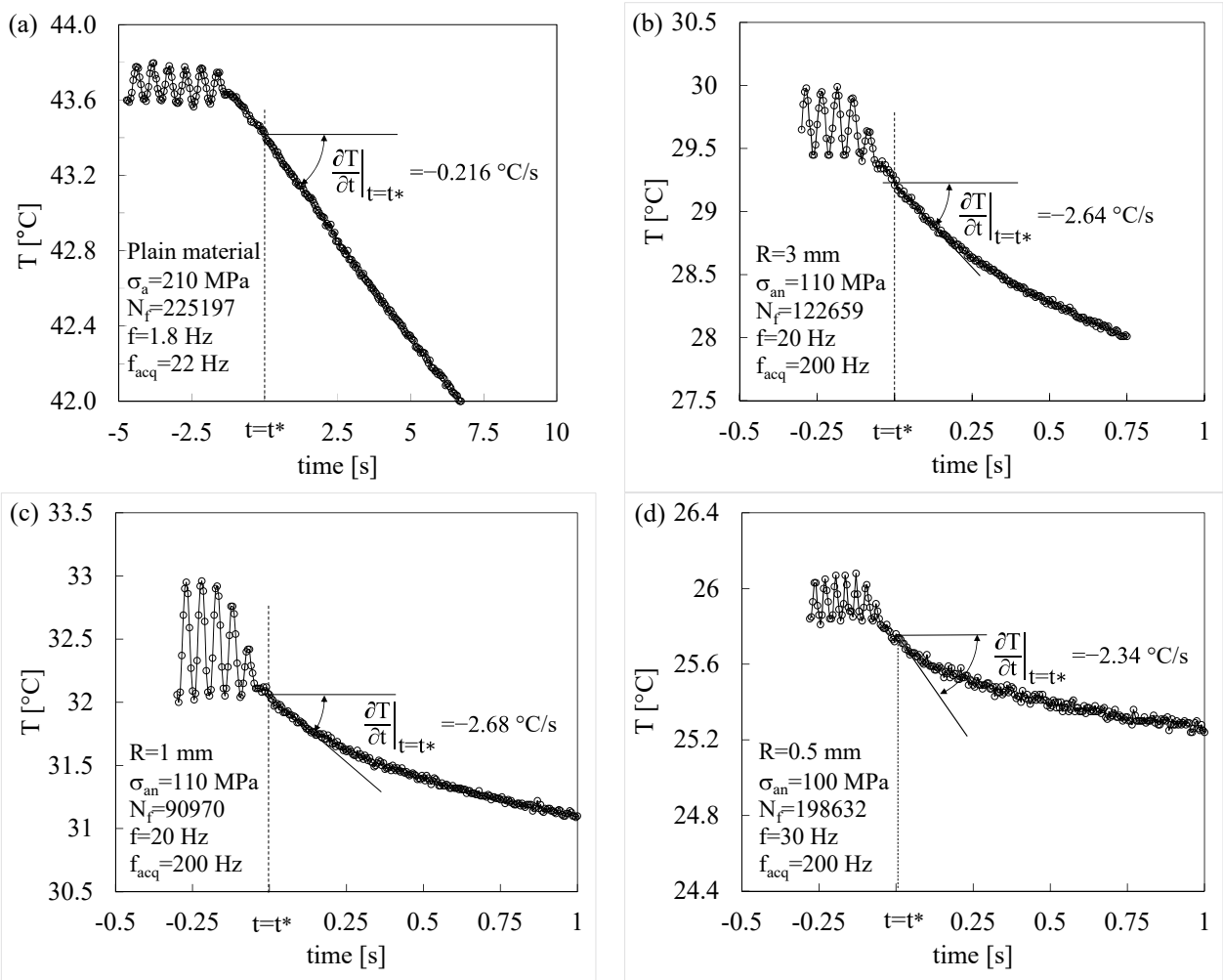

Fig. 6. Typical cooling gradients measured during the fatigue tests carried out for different specimens' geometry.

Conversely, in the case of notched specimens, the time window is approximately some tenths of a second and the corresponding temperature variations are limited to few tenths of a degree. It is worth noting that, concerning

notched specimens, t* was define, having in hand the signal acquired from the load cell test machine. In this paper, the Q parameter was calculated by considering the maximum temperature measured in an area embracing the notch, as will be discussed in the next section.

According to Meneghetti (2006), the fatigue test results of plain specimens were reanalysed in terms of the characteristic value of the specific heat loss per cycle Q measured at 50% of the number of cycles to specimen's failure, N_f. Concerning the notched specimens, the Q value measured before crack initiation was assumed as characteristic value. Fig. 4b shows that the scatter band shown in Fig. 2, published by Meneghetti et al (2013), successfully correlated all new fatigue data with those obtained previously on sharper notches.

5. Discussion

In view of extending of the heat energy-based approach to severely notched specimens, in order to account for the notch support effect under fatigue loading, Meneghetti and Ricotta (2016) have recently defined a theoretical frame and the corresponding experimental procedure to measure the specific heat loss Q averaged over a volume V surrounding the tip of a fatigue crack, the averaged energy parameter being defined as Q*. For rounded V-notches under Mode I loading, the size of the control volume may be defined for example according to Lazzarin and Berto (2005). Considering Fig. 7a, the dimension of the control volume V is related to the opening angle 2α, the notch radius R and the material-dependent distance R_c, that can be calculated according to Lazzarin and Zambardi (2001):

$$R_C = \frac{(1+\nu)(5-8\nu)}{4\pi} \cdot \left(\frac{\Delta K_{th}}{2 \cdot \sigma_{A,-1}} \right)^2 \tag{3}$$

For the material analysed here, R_c was found equal to 0.126 mm. Considering specimens having R=0.5 mm, V is equal to 0.260 mm^3, according to Fig 7b. Due to this very limited value, it was found that for the material and notch geometry, the difference between Q and Q* was lower than 10%. Therefore, energy-averaging was not performed and Q* was approximated with Q, evaluated from the maximum temperature measured by the infrared camera inside an area embracing the notch (see the white circle in Fig 7b).

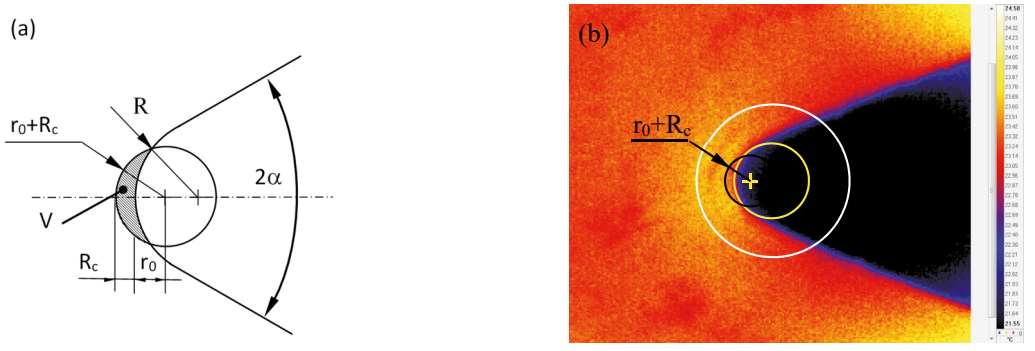

Fig. 7. Definition of a) control volume determined according to Lazzarin and Berto (2005) and b) example of application in the case of R=0.5 mm (σ_a=90 MPa, N_f=342070, f=20 Hz).

6. Conclusions

The fully reversed axial fatigue behavior of 4-mm-thick AISI 304L notched specimens was investigated in terms of specific heat loss per cycle, Q, which can be easily evaluated at the notch tip starting from temperature measurements performed during the fatigue tests. As compared to previous measurements performed by means of thin wires copper-constantan thermocouples, an infrared camera equipped with an extender ring was used in the present work, which increased the spatial resolution of the thermal measurements up to approximately 23 μm/pixel. Thanks to the adopted experimental set-up, three notch radii smaller than those considered in previous papers could

be analysed here, namely R=0.5, 1 and 3 mm. The specific heat loss per cycle evaluated at the notch tip was seen to correlate all present fatigue test results with those previously generated both from notches with larger notch tip radii (namely 3, 5 and 8 mm) and from plain specimens. Interestingly, experimental measurements demonstrated that the specific heat loss measured at the notch tip was practically equal to that averaged inside a properly defined structural volume of the material. It is the authors' opinion that additional work is needed on this topic.

Acknowledgements

This work was carried out as a part of the project CODE CPDA145872 of the University of Padova. The Authors would like to express their gratitude for financial support.

References

Curà, F., Curti, G., Sesana, R., 2005. A new iteration method for the thermographic determination of fatigue limit in steels. International Journal of Fatigue 27, 453-459.

Curà, F., Gallinatti, AE., Sesana, R., 2012. Dissipative aspects in thermographic methods. Fatigue and Fracture of Engineering Materials and Structures, 35, 1133-1147.

Curti, G., Geraci, AL., Risitano, A., 1989. A new method for rapid determination of the fatigue limit. Ingegneria Automotoristica 42, 634–636. in italian.

Dengel, D., Harig, H., 1980. Estimation of the fatigue limit by progressively-increasing load tests. Fatigue and Fracture of Engineering Materials and Structures 3, 113-128.

El Haddad, M. H., Topper, T. H. and Smith, K. N., 1979. Fatigue crack propagation of short cracks. Journal of Engineering Materials and Technology (ASME Trans.) 101, 42–45.

Fargione, G., Geraci, A., La Rosa, G., Risitano, A., 2002. Rapid determination of the fatigue curve by the thermographic method. International Journal of Fatigue 24, 11-19.

Fan, J., Guo, X., Wu, C., 2012. A new application of the infrared thermography for fatigue evaluation and damage assessment. International Journal of Fatigue 44, 1-7.

Jegou, L., Marco, Y., Le Saux, V., Calloch, S., 2013. Fast prediction of the Wöhler curve from heat build-up measurements on Short Fiber Reinforced Plastics. International Journal of Fatigue 47, 259-267.

Jones, R., Krishnapillai, M., Cairns, K., Matthews, N., 2010. Application of infrared thermography to study crack growth and fatigue life extension procedures. Fatigue and Fracture of Engineering Materials and Structures 33, 871–884.

La Rosa, G., Risitano, A., 2000. Thermographic methodology for rapid determination of the fatigue limit of materials and mechanical components. International Journal of Fatigue 22, 65-73.

Lazzarin, P., Zambradi, R., 2001. A finite-volume-energy based approach to predict the static and fatigue behavior of component with sharp V-shaped notches. International Journal of Fracture 112, 275-298.

Lazzarin, P., Berto, F., 2005. Some expressions for the strain energy in a finite volume surrounding the root of blunt V-notches. International Journal of Fracture 135, 161-185.

Luong, MP., 1995. Infrared thermographic scanning of fatigue in metals. Nuclear Engineering Design 158, 363-376.

Meneghetti, G., 2007. Analysis of the fatigue strength of a stainless steel based on the energy dissipation. International Journal of Fatigue 29, 81-94.

Meneghetti, G., Ricotta, M., 2012. The use of the specific heat loss to analyse the low- and high-cycle fatigue behaviour of plain and notched specimens made of a stainless steel. Engineering Fracture Mechanics 81, 2-17.

Meneghetti, G., Ricotta, M., Atzori, B., 2013. A synthesis of the push-pull fatigue behaviour of plain and notched stainless steel specimens by using the specific heat loss. Fatigue and Fracture of Engineering Materials and Structures 36, 1306–1322.

Meneghetti, G., Ricotta, M., Negrisolo, L., Atzori, B., 2014. A synthesis of the fatigue behavior of stainless steel bars under fully reversed axial or torsion loading by using the specific heat loss. Key Engineering Materials 577–578, 453–6.

Maneghetti, G., Ricotta, M., 2016. Evaluating the heat energy dissipated in a small volume surrounding the tip of a fatigue crack. International Journal of Fatigue, *in press, http://dx.doi.org/10.1016/j.ijfatigue.2016.04.001.*

Plekhov, O., Palin-Luc, T., Saintier, N., Uvarov, S., Naimark, O., 2005. Fatigue crack initiation and growth in a 35CrMo4 steel investigated by infrared thermography. Fatigue and Fracture of Engineering Materials and Structures 28, 169–178.

Reifsnider, KL., Williams, RS., 1974. Determination of fatigue-related heat emission in composite materials. Experimental Mechanics, 14, 479-485.

Risitano, A., Risitano, G., 2013. Cumulative damage evaluation in multiple cycle fatigue tests taking into account energy parameters, International Journal of Fatigue 48, 214–222.

Starke, P., Walther, F., Eifler, D., 2007. Fatigue assessment and fatigue life calculation of quenched and tempered SAE 4140 steel based on stress–strain hysteresis, temperature and electrical resistance measurements. Fatigue and Fracture of Engineering Materials and Structures 30, 1044–1051.

Ummenhofer, T., Medgenberg, J., 2009. On the use of infrared thermography for the analysis of fatigue damage process in welded joints. International Journal of Fatigue 31, 130-137.